Inorganic Chemistry

Article

pubs.acs.org/IC

An Asymmetrically Derivatized 1,2,3-Triphospholide: Synthesis and Reactivity of the 4-(2′-Pyridyl)-1,2,3-triphospholide Anion

Robert S. P. Turbervill and Jose M. Goicoechea*

Department of Chemistry, University of Oxford, Chemistry Research Laboratory, Mansfield Road, Oxford OX1 3TA, United Kingdom

Supporting Information

ABSTRACT: Reactions between anionic heptaphosphide clusters ($[P_7]^{3-}$/$[HP_7]^{2-}$) and 2-ethynylpyridine yielded the 4-(2′-pyridyl)-1,2,3-triphospholide anion ($[P_3C_2H(2\text{-}C_5H_4N)]^-$; **1**). This species was isolated as a compositionally pure $[K(2,2,2\text{-crypt})]^+$ salt in moderate yields. Preliminary coordination studies of **1** toward $Mo(CO)_6$ or $Mo(py)_3(CO)_3$ (py = pyridine) afforded the diamagnetic piano-stool complex $[\{\eta^5\text{-}P_3C_2H(2\text{-}C_5H_4N)\}Mo(CO)_3]^-$ (**2**). By contrast, reaction of **1** with $Mo(COD)(CO)_4$ (COD = 1,5-cyclooctadiene) yielded $[\{\kappa^2P,N\text{-}P_3C_2H(2\text{-}C_5H_4N)\}Mo(CO)_4]^-$ (**3**) which readily loses a carbonyl on heating to give **2**. Reaction of **2** with $Mo(COD)(CO)_4$ afforded the bimetallic system $[\{\mu{:}\eta^5,\kappa^2P,N\text{-}P_3C_2H(2\text{-}C_5H_4N)\}\{Mo(CO)_3\}\{Mo(CO)_4\}]^-$ (**4**).

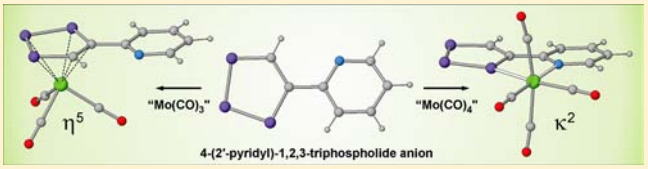

INTRODUCTION

The isolobal relationship between methine groups (C−H) and phosphorus has frequently been employed to design organophosphorus molecules in which one or several C−H fragments have been replaced by phosphorus atoms. The diagonal relationship between carbon and phosphorus (a result of the competing effects of descending and traversing the periodic table from left to right) has led to phosphorus being nicknamed "the carbon copy".[1] However, despite their similarities (comparable covalent radii and electronegativities), the synthesis of specific phosphorus-containing analogues of organic or organometallic molecules can often be fraught with difficulty, in large part due to the reluctance of heavier p-block elements to form multiple bonds.

Of the limitless number of "phospha-organic" molecules that are conceivable, the 6π electron phospholides $[P_n(CH)_{5-n}]^-$ (n = 1−5) have received a great deal of attention in the chemical literature. Their isolobal relationship with the cyclopentadienyl anion (a staple of organometallic chemistry) has led to extensive fundamental and applied studies on these types of ligand systems. Research on mono- and diphospholide ligands make up the bulk of research that has been carried out in this area.[2] The majority of studies on triphospholides have centered on the synthesis and coordination chemistry of the 1,2,4-isomers, typically accessed by the chemical reduction of phospha-alkynes.[3] This method also produces 1,3-diphospholides in an equimolar ratio; however, the products can frequently be separated through fractional crystallization. To date, a number of complexes of 1,2,4-triphospholides have been characterized for elements of the main-group,[4] d-,[5] and f-blocks.[6] The 1,2,3-triphospholide isomer, by contrast, has been more elusive. Until recently only three such species could be isolated in compositionally pure samples (either as free anions or coordinated to metal atoms), namely $[P_3C_2H_2]^-$, $[P_3C_2H(C_6H_5)]^-$, and $[P_3C_2(C_6H_5)_2]^-$.[7−9] While these species represent remarkable breakthroughs in main-group chemistry, they can only be isolated in the immediate coordination sphere of a transition metal or after challenging multistep syntheses. In 2008 two separate syntheses of the triphospholide analogue of the indenyl anion were also reported.[10,11] More recently, our research group observed that the chemical reaction of trianionic heptapnictide cages, $[E_7]^{3-}$ (E = P, As), with acetylene can be used to isolate compositionally pure samples of the protio tripnictolide anions $[E_3C_2H_2]^-$.[12]

Building on this research, we can now report the isolation of an asymmetrically substituted 1,2,3-triphospholide anion, the 4-(2′-pyridyl)-1,2,3-triphospholide species, $[P_3C_2H(2\text{-}C_5H_4N)]^-$ (**1**), obtained by reaction of **2**-ethynylpyridine with K_3P_7 (or with salts of the protonated dianion $[HP_7]^{2-}$). This pro-chiral anion has a rich coordination chemistry that we have exploited to yield a variety of novel metal complexes.

EXPERIMENTAL DETAILS

General Synthetic Methods. All reactions and product manipulations were carried out under an inert atmosphere of argon or dinitrogen using standard Schlenk-line or glovebox techniques (MBraun UNIlab glovebox maintained at <0.1 ppm H_2O and <0.1 ppm O_2). The Zintl phase precursor K_3P_7 was synthesized according to a previously reported synthetic procedure from a mixture of the elements (K, 99.95%, Strem; P, 99.99%, Sigma-Aldrich).[13] 2,2,2-Crypt (4,7,13,16,21,24-hexaoxa-1,10-diazabicyclo[8,8,8]-hexacosane; VWR, 99%) was used as received after careful drying under vacuum. Tricarbonyltris(pyridine)molybdenum ($Mo(py)_3(CO)_3$) and tetracarbonyl(1,5-cyclooctadiene)molybdenum ($Mo(1,5\text{-}COD)(CO)_4$) were prepared according to previously reported procedures.[14,15] 2-Ethynylpyridine (98%, Sigma-Aldrich) was used as

Received: February 20, 2013
Published: April 22, 2013

   dx.doi.org/10.1021/ic400448x | Inorg. Chem. 2013, 52, 5527−5534

received. Hexanes (hex; 99+%, Rathburn), pentane (HPLC grade, Sigma-Aldrich), diethylether (99.9% stabilized with copper gauze, Fischer), and dimethylformamide (DMF; 99.9%, Rathburn) were purified using an MBraun SPS-800 solvent system. Tetrahydrofuran (THF; 99.9%, Rathburn) was distilled over a sodium metal/benzophenone mixture. d_8-THF (Sigma-Aldrich, 99.5%) and CD_2Cl_2 (Euriso-Top, 99.9%) were dried over CaH_2 and vacuum distilled before use. All dry solvents were stored under argon in gastight ampules. Additionally, hexanes, pentane diethylether, and THF were stored over activated 3 Å molecular sieves.

Synthesis of [K(2,2,2-crypt)][1] (1: $P_3C_2H(2\text{-}C_5H_4N)]^-$). 2-Ethynylpyridine (58 μL, 0.573 mmol) was added dropwise to a stirring solution of $[K(2,2,2\text{-crypt})]_2[HP_7]$ (200 mg, 0.19 mmol) in DMF (3 mL), resulting in an instant color change of the reaction mixture to a deep purple. The solution was stirred overnight. The solvent was removed under dynamic vacuum to yield a deep purple oily solid, which was partially redissolved in THF (10 mL). Air was then bubbled through the solution for 2 min (in order to oxidize undesired radical side-products), which resulted in an instant color change to orange-brown, and the formation of a pale precipitate. The solution was then filtered, and the THF removed under dynamic vacuum to give a brown-orange oil. The solid sample was washed with diethylether (10 mL) yielding a peach solid (81.2 mg, 30%). Crystals suitable for single crystal X-ray diffraction were grown by slow diffusion of hexanes (20 mL) into a THF (5 mL) solution of the product (CCDC-918948). Anal. Calcd for $C_{25}H_{41}KN_3O_6P_3$: C, 49.09; H, 6.76; N, 6.87. Found: C, 49.62; H, 6.54; N, 6.82. ^{1}H NMR (500 MHz, d_8-THF, 20 °C): δ (ppm) 9.88 (ddd, 1H, $^2J_{H-P}$ = 47 Hz, $^3J_{H-P}$ = 13 Hz, $^3J_{H-P}$ = 7 Hz, C*H* of phospholide; for a full analysis of the spin system see Supporting Information, Table S5), 8.39 (m, 1H, C*H* of pyridyl), 8.20 (m, 1H, C*H* of pyridyl), 7.42 (m, 1H, C*H* of pyridyl), 6.79 (m, 1H, C*H* of pyridyl), 3.48 (s, 12H, 2,2,2-crypt), 3.45 (t, 12H, $^3J_{H-H}$ = 5 Hz, 2,2,2-crypt), 2.45 (t, 12H, $^3J_{H-H}$ = 5 Hz, 2,2,2-crypt). ^{1}H{^{31}P} NMR (500 MHz, d_8-THF, 20 °C): δ (ppm) 9.88 (s, 1H, C*H* of phospholide), the rest of the resonances observed are as detailed above. ^{31}P NMR (202.4 MHz, d_8-THF, 20 °C): δ (ppm) 293.1 (m, 1P, $^1J_{P-P}$ = −462 Hz, $^1J_{P-P}$ = −505 Hz, P2), 278.3 (m, 1P, $^2J_{P-P}$ = 13 Hz, P3), 274.3 (m, 1P, P1). ^{13}C{^{1}H} NMR (125.8 MHz, d_8-THF, 20 °C): δ (ppm) 177.3 (m, *ipso* C of py), 162.3 (m, *C*py of phospholide), 161.3 (m, *C*H of phospholide), 149.5 (s, pyridyl), 135.5 (s, pyridyl), 123.6 (s, pyridyl), 118.7 (s, pyridyl), 71.5 (s, 2,2,2-crypt), 68.7 (s, 2,2,2-crypt), 55.0 (s, 2,2,2-crypt). ESI-MS (−ve ion mode, DMF): *m*/*z* 195.9 $[P_3C_2H(C_5H_4N)]^-$. ESI-MS (+ve ion mode, DMF): *m*/*z* 1025.8 $\{[K(2,2,2\text{-crypt})]_2[P_3C_2H(C_5H_4N)]\}^+$.

Synthesis of [K(2,2,2-crypt)][2] (2: $[\{\eta^5\text{-}P_3C_2H(2\text{-}C_5H_4N)\}Mo(CO)_3]^-$). A mixture of [K(2,2,2-crypt)][**1**] (20.4 mg, 32.8 μmol) and $Mo(py)_3(CO)_3$ (8.7 mg, 32.8 μmol) were weighed into an NMR tube equipped with a gastight valve. d_8-THF (0.5 mL) was added and the tube sealed and agitated to mix the contents. It was then heated to 70 °C for 2 h, after which ^{1}H and ^{31}P NMR spectroscopy indicated full conversion to the product. The orange solution was transferred into a Schlenk tube under argon and solvent removed under vacuum yielding an orange oil which was washed with diethyl ether (3 × 2 mL) and dried under vacuum yielding the product, [K(2,2,2-crypt)][**2**], as an orange-yellow powder. Yield 23.8 mg (92%). Crystals suitable for single crystal X-ray diffraction were grown by slow diffusion of hexanes (20 mL) into a THF (5 mL) solution of the product (CCDC-918949). Anal. Calcd for $MoC_{28}H_{41}KN_3O_9P_3$: C, 42.48; H, 5.22; N, 5.31. Found: C, 43.10; H, 5.37; N, 5.15. ^{1}H NMR (500 MHz, d_8-THF, 20 °C): δ (ppm) 8.24 (1H, m, C*H* of pyridyl), 7.61 (1H, m, C*H* of pyridyl), 7.42 (1H, m, C*H* of pyridyl), 6.88 (1H, overlapping m, C*H* of pyridyl), 6.84 (1H, ddd, $^2J_{H-P}$ = 43 Hz, $^3J_{H-P}$ = 11 Hz, $^3J_{H-P}$ = 4 Hz, C*H* of phospholide; for a full spin system analysis see Table S6), 3.58 (12H, s, 2,2,2-crypt), 3.54 (12H, t, $^3J_{H-H}$ = 5 Hz, 2,2,2-crypt), 2.56 (12H, t, 2,2,2-crypt). ^{1}H{^{31}P} NMR (500 MHz, d_8-THF, 20 °C): δ (ppm) 6.84 (s, 1H, C*H* of phospholide). ^{31}P NMR (202.4 MHz, d_8-THF, 20 °C): δ (ppm) 77.6 (m, 1P, $^1J_{P-P}$ = −438 Hz, $^2J_{P-P}$ = 13 Hz, P3), 70.8 (m, 1P, $^1J_{P-P}$ = −400 Hz, P1), 42.4 (m, 1P, P2). ^{13}C{^{1}H} NMR 125.8 MHz, d_8-THF, 20 °C): δ (ppm) 228.2 (s, *C*O), 160.6 (dd, $^2J_{C-P}$ = 22 Hz, $^3J_{C-P}$ = 4 Hz, ipso *C* of pyridyl), 148.7 (s, pyridyl), 135.7 (s, pyridyl), 134.3 (ddd, $^1J_{C-P}$ = −83 Hz, $^2J_{C-P}$ = −11 Hz, $^2J_{C-P}$ = −6 Hz, *C*py of phospholide), 123.6 (d, $^3J_{C-P}$ = 12 Hz, pyridyl), 120.8 (s, pyridyl), 114.9 (ddd, $^1J_{C-P}$ = −83 Hz, $^2J_{C-P}$ = −8 Hz, $^2J_{C-P}$ = −3.5 Hz, *C*H of phospholide), 71.2 (s, 2,2,2-crypt), 68.4 (s, 2,2,2-crypt), 54.7 (s, 2,2,2-crypt). ESI-MS (−ve ion mode, DMF): *m*/*z* 378.5 $[\{P_3C_2H(C_5H_4N)\}Mo(CO)_3]^-$. ESI-MS (+ve ion mode DMF): *m*/*z* 1210.0 $\{[K(2,2,2\text{-crypt})]_2[\{P_3C_2H(C_5H_4N)\}Mo(CO)_3]\}^+$. IR ν_{CO} (cm^{-1}): 1924, 1828, 1812.

Synthesis of [K(2,2,2-crypt)][3] (3: $[\{\kappa^2P,N\text{-}P_3C_2H(2\text{-}C_5H_4N)\}Mo(CO)_4]^-$). A mixture of **1** (20.3 mg, 32.8 μmol) and Mo(1,5-COD)$(CO)_4$ (10.3 mg, 32.8 μmol) were weighed into an NMR tube equipped with a gastight valve. CD_2Cl_2 (0.5 mL) was added and the tube sealed and agitated to mix the contents. The reaction was then left at room temperature, and regularly monitored by NMR spectroscopy, showing the disappearance of resonances arising due to **1** with concomitant growth of resonances assigned to **3**. After 48 h there was approximately 85% of **3**, alongside approximately 10% (by integration) of the η^5 complex (**2**) and 5% of **1**. After characterization by multielement NMR spectroscopy, the red-brown solution was layered with pentane and placed in a freezer at −35 °C. Crystals suitable for single crystal X-ray diffraction grew after a few days (CCDC-918950). This reaction may also be performed in d_8-THF; however, conversion to the η^5 complex (**2**) occurs much more rapidly in this solvent and all attempts to grow crystals were unsuccessful. Anal. Calcd for $MoC_{29}H_{41}KN_3O_{10}P_3$: C, 42.50; H, 5.04; N, 5.13. Found: C, 42.72; H, 5.03; N, 5.08. ^{1}H NMR (500 MHz, d_8-THF, 20 °C): δ (ppm) 9.51 (1H, ddd, $^2J_{H-P}$ = 44 Hz, $^3J_{H-P}$ = 28 Hz, $^3J_{H-P}$ = 4 Hz, C*H* of phospholide; for a full analysis of the spin system see Table S7), 9.02 (1H, m, C*H* of pyridyl), 8.00 (1H, m, C*H* of pyridyl), 7.69 (1H, m, C*H* of pyridyl), 6,82 (1H, m, C*H* of pyridyl), 3.52 (12H, s, 2,2,2-crypt), 3.46 (12H, t, $^3J_{H-H}$ = 5 Hz, 2,2,2-crypt), 2.47 (12H, t, 2,2,2-crypt). ^{1}H{^{31}P} NMR (500 MHz, d_8-THF, 20 °C): δ (ppm) 9.51 (s, 1H, C*H* of phospholide). ^{31}P NMR (202.4 MHz, d_8-THF, 20 °C): δ (ppm) 266.6 (m, 1P, $^1J_{P-P}$ = −453 Hz, $^2J_{P-P}$ = 25 Hz, P1), 262.5 (m, 1P, $^1J_{P-P}$ = −585 Hz, P3), 240.2 (m, 1P, P2). ^{13}C{^{1}H} NMR (125.8 MHz, d_8-THF, 20 °C): δ (ppm) 223.5 (d, $^2J_{C-P}$ = −6 Hz, *C*O trans to N), 221.1 (dd, $^2J_{C-P}$ = 34 Hz, $^3J_{C-P}$ = 3 Hz, *C*O trans to P), 207.4 (d, $^2J_{C-P}$ = −11 Hz, axial *C*O), 168.8 (m, *C*py of phospholide), 156.9 (m, *C*H of phospholide), 156.3 (s, pyridyl), 149.5 (m, *ipso* C), 137.6 (s, pyridyl), 120.9 (d, $^2J_{C-P}$ = 9 Hz, pyridyl), 118.9 (s, pyridyl), 71.1 (s, 2,2,2-crypt), 68.3 (s, 2,2,2-crypt), 54.6 (s, 2,2,2-crypt). ESI-MS (−ve ion mode DMF): *m*/*z* 406.0 $[\{P_3C_2H(C_5H_4N)\}Mo(CO)_4]^-$. IR ν_{CO} (cm^{-1}): 2004, 1895, 1879, 1828.

Synthesis of [K(2,2,2-crypt)][4] (4: $[\{\mu\text{:}\eta^5,\kappa^2P,N\text{-}P_3C_2H(2\text{-}C_5H_4N)\}\{Mo(CO)_3\}\{Mo(CO)_4\}]^-$). A mixture of **1** (20.4 mg, 32.8 μmol) and $Mo(py)_3(CO)_3$ (8.8 mg, 32.8 μmol) were weighed out into a Schlenk tube, dissolved in THF (1 mL) and heated at 70 °C under argon for 2 h. The bright orange solution was then filtered, and the solvent removed under dynamic vacuum to yield an orange solid. The solid was redissolved in CD_2Cl_2 (0.5 mL); ^{1}H and ^{31}P NMR spectroscopy indicated quantitative conversion to **2**. To this solution Mo(COD)$(CO)_4$ (10.3 mg, 32.8 μmol) was added, and the NMR tube was heated to 40 °C for 1 h, at which point ^{1}H and ^{31}P NMR spectroscopy showed the formation of a new complex. After characterization by multielement NMR spectroscopy the intensely colored orange solution was filtered into a Schlenk tube and layered with pentane yielding a yellow oil. Anal. Calcd for $Mo_2C_{32}H_{41}KN_3O_{13}P_3$: C, 38.45; H, 4.13; N, 4.20. Found: C, 38.89; H, 4.07; N, 4.24. ^{1}H NMR (500 MHz, CD_2Cl_2, 20 °C): δ (ppm) 8.86 (1H, m, C*H* of pyridyl), 7.61 (1H, m, C*H* of pyridyl), 7.43 (1H, m, C*H* of pyridyl), 6.89 (1H, m, C*H* of pyridyl), 6.68 (ddd, $^2J_{H-P}$ = 40 Hz, $^3J_{H-P}$ = 16 Hz, $^3J_{H-P}$ = 3 Hz, 1H, C*H* of phospholide; for a full analysis of the spin system see Table S8), 3.57 (s, 1H, 2,2,2-crypt), 3.51 (t, $^3J_{H-H}$ = 5 Hz, 1H, 2,2,2-crypt), 2.52 (t, 1H, 2,2,2-crypt). ^{1}H{^{31}P} NMR (500 MHz, CD_2Cl_2, 20 °C): δ (ppm) 6.68 (s, 1H, C*H* of phospholide). ^{31}P NMR (202.4 MHz, CD_2Cl_2, 20 °C): δ (ppm) 119.4 (m, $^1J_{P-P}$ = −546 Hz, $^2J_{P-P}$ = 21 Hz, 1P, P3), 63.5 (m, $^1J_{P-P}$ = −384 Hz, 1P, P1), −21.7 (m, 1P, P2). ^{13}C{^{1}H} NMR (125.8 MHz, CD_2Cl_2, 20 °C): δ (ppm) 226.2 (s, CO of $Mo(CO)_3$), 222.3 (d, $^2J_{C-P}$ = −7 Hz, CO trans to N), 217.7 (dd, $^2J_{C-P}$ = 41 Hz, $^3J_{C-P}$ = 2 Hz, CO

dx.doi.org/10.1021/ic400448x | Inorg. Chem. 2013, 52, 5527−5534

Table 1. Selected X-ray Data Collection and Refinement Parameters for [K(2,2,2-crypt)][1], [K(2,2,2-crypt)][2], and [K(2,2,2-crypt)][3]·0.5CH_2Cl_2

	[K(2,2,2-crypt)][**1**]	[K(2,2,2-crypt)][**2**]	[K(2,2,2-crypt)][**3**]·0.5CH_2Cl_2
formula	$C_{25}H_{41}KN_3O_6P_3$	$C_{28}H_{41}KMoN_3O_9P_3$	$C_{29.5}H_{42}ClKMoN_3O_{10}P_3$
fw (g mol^{-1})	611.62	791.59	862.06
cryst syst	monoclinic	orthorhombic	monoclinic
space group	$P2_1/c$	$Cmca$	$P2_1/n$
a (Å)	13.0560(3)	20.7468(4)	11.5991(1)
b (Å)	11.9141(2)	16.2409(3)	22.5642(1)
c (Å)	20.1168(3)	20.7960(3)	14.9144(1)
α (deg)			
β (deg)	101.273(2)		97.709(1)
γ (deg)			
V (Å^3)	3068.81(10)	7007.1(2)	3868.18(5)
Z	4	8	4
radiation, λ (Å)	Cu Kα, 1.541 78	Cu Kα, 1.541 78	Cu Kα, 1.541 78
T (K)	150	150	150
ρ_{calcd} (g cm^{-3})	1.324	1.501	1.480
μ (mm^{-1})	3.344	5.873	6.010
reflns collected	14 416	18 413	82 775
indep reflns	5394	3745	8092
params	343	231	473
R(int)	0.0308	0.0258	0.0291
R1/wR2,[a] $I \geq 2\sigma_I$ (%)	4.94/13.87	2.85/7.15	2.64/6.89
R1/wR2,[a] all data (%)	5.85/14.60	3.23/7.51	2.77/7.01
GOF	1.082	1.047	1.029

[a] $R1 = [\Sigma||F_o| - |F_c||]/\Sigma|F_o|$; $wR2 = \{[\Sigma w[(F_o)^2 - (F_c)^2]^2]/[\Sigma w(F_o^2)^2]\}^{1/2}$; $w = [\sigma^2(F_o)^2 + (AP)^2 + BP]^{-1}$, where $P = [(F_o)^2 + 2(F_c)^2]/3$ and the A and B values are 0.0884 and 0.89 for [K(2,2,2-crypt)][**1**], 0.0417 and 8.02 for [K(2,2,2-crypt)]**2**, and 0.0347 and 2.61 for [K(2,2,2-crypt)][**3**]·0.5CH_2Cl_2.

trans to P), 206.2 (d, $^2J_{C-P} = -10$ Hz, axial CO), 205.2 (d, $^2J_{C-P} = -11$ Hz, axial CO), 160.7 (d, $^2J_{C-P} = 22$ Hz, ipso *C* of pyridyl), 155.8 (m, Cpy of phospholide), 148.6 (s, pyridyl), 137.7 (s, pyridyl), 121.6 (d, $^3J_{C-P} = 8$ Hz, pyridyl), 121.0 (s, pyridyl), 109.8 (dd, $^1J_{C-P} = -89$ Hz, $^2J_{C-P} = -9$ Hz, *C*H of phospholide), 70.9 (2,2,2-crypt), 68.0 (2,2,2-crypt), 28.4 (2,2,2-crypt). ESI-MS (−ve ion mode DMF): m/z 584.3 ($[\{P_3C_2H(2\text{-}C_5H_4N)\}Mo_2(CO)_7\}]^-$), 556.2 ($[\{P_3C_2H(2\text{-}C_5H_4N)\}Mo_2(CO)_6\}]^-$). IR ν_{CO} (cm^{-1}): 2020, 1940, 1912, 1884, 1847.

Single Crystal X-ray Structure Determination. Single-crystal X-ray diffraction data were collected using an Oxford Diffraction Supernova dual-source diffractometer equipped with a 135 mm Atlas CCD area detector. Crystals were selected under Paratone-N oil, mounted on micromount loops, and quench-cooled using an Oxford Cryosystems open flow N_2 cooling device.[16] Data were collected at 150 K using mirror monochromated Cu Kα radiation (λ = 1.5418 Å) and processed using the CrysAlisPro package, including unit cell parameter refinement and interframe scaling (which was carried out using SCALE3 ABSPACK within CrysAlisPro).[17] Equivalent reflections were merged and diffraction patterns processed with the CrysAlisPro suite. Structures were subsequently solved using direct methods, and refined on F^2 using the SHELXL 97-2 package.[18] A table of selected data collection and refinement parameters is provided in Table 1.

Other Characterization Techniques. ^{1}H, ^{13}C, and ^{31}P NMR spectra were acquired at 500, 125.8, and 202.4 MHz, respectively, on a Bruker AVIII 500 MHz NMR spectrometer. ^{1}H and ^{13}C spectra are reported relative to TMS and were referenced to the most downfield residual solvent resonance (d_8-THF: δ_H 3.58 ppm, δ_C 67.2 ppm; CD_2Cl_2; δ_H 5.32 ppm, δ_C 53.8 ppm). ^{31}P spectra were externally referenced to 85% H_3PO_4 (δ_P 0 ppm). Spectral simulations were carried out using the program gNMR.[19] All coupling constant data provided in this manuscript are for the fitted simulated spectra starting from experimentally and computationally determined J values. Full tables of NMR data for all of the compounds described are provided below.

Positive and negative ion mode electrospray mass spectra were recorded on DMF solutions of the compounds (10−20 μM) on a Waters LCT time of flight mass spectrometer with a Z-spray source (150 °C source temperature, 200 °C desolvation temperature, 2.4 kV capillary voltage, and 25 V cone voltage). The samples were made up inside a glovebox under an inert atmosphere and rapidly transferred to the spectrometer in an airtight syringe. Samples were introduced directly with a 1 mL SGE syringe and a syringe pump at 0.6 mL h^{-1}.

IR data were recorded on solid samples in Nujol mulls. The mulls were made up inside an inert-atmosphere glovebox and the KBr plates placed in an airtight sample holder prior to data collection. Spectra were recorded on a Thermo Scientific Nicolet iS5 FT-IR spectrometer in absorbance mode.

Transmission powder X-ray patterns were recorded using a Siemens D5000 diffractometer in modified Debye−Scherrer geometry equipped with an MBraun position sensitive detector. The instrument produced Cu Kα1 radiation (λ = 1.540 56 Å) using a germanium monochromator and a standard Cu source. Data were recorded on samples in flame-sealed capillaries under dinitrogen. The capillaries were mounted on a goniometer head and aligned so that rotation occurred along the long central axis of the capillary. During a measurement the capillary was rotated at 60 rpm to minimize any preferred orientation effects that might occur.

Computational Details. Geometry optimizations on **1**−**4** were performed using the Amsterdam Density Functional package (ADF2012.01).[20] A triple-ζ Slater-type basis set, extended with a double polarization function (TZ2P), was used to describe all atoms. The local density approximation was employed for the optimizations,[21] along with the local exchange-correlation potential of Vosko, Wilk, and Nusair,[22] and the gradient corrections to exchange and correlation proposed by Becke and Perdew (BP86).[23] Relativistic effects were incorporated using the zeroth order relativistic approximation (ZORA).[24] The presence of cations in the crystal lattice was modeled by surrounding the anion with a continuum dielectric using COSMO.[25] The chosen dielectric constant ε = 7.58 corresponds to that of tetrahydrofuran, although structural parameters

dx.doi.org/10.1021/ic400448x | Inorg. Chem. 2013, 52, 5527−5534

are not strongly dependent on this choice. All structures were optimized using the gradient algorithm of Versluis and Ziegler.[26]

The signs associated with the spin−spin coupling constants (J) for all complexes were determined by computing Fermi contact values using the Gaussian09 program package revision A02.[27] The B3PW91 functional[28] was employed along with the 6-311++G (2d, 2p) basis set for all of the light atoms (H, C, N, O, P).[29] The 3-21G basis set was used to describe the molybdenum atoms in **2**−**3** (the nature of the basis set used to describe molybdenum had no effect on the computed signs of the spin−spin coupling constants).[30] Initial atomic coordinates were taken from single-crystal X-ray diffraction experiments for **1**−**3**. The coordinates for **4** were taken from the optimized computed geometry of the anion.

RESULTS AND DISCUSSION

Reaction of $[K(2,2,2\text{-crypt})]_2[HP_7]$ with 3 equiv of 2-ethynylpyridine in DMF gives rise to a dark purple solution which upon removal of the solvent under a dynamic vacuum affords a purple oil. A compositionally pure peach sample of $[K(2,2,2\text{-crypt})][\mathbf{1}]$ can be extracted from solution after aerial oxidation in moderate yields (approximately 30%) using THF. Single crystal X-ray diffraction quality crystals of $[K(2,2,2\text{-crypt})][\mathbf{1}]$ were obtained by slow diffusion of hexanes into a THF solution of the product (Figure 1). Selected data

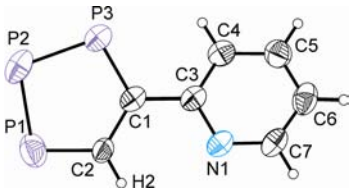

Figure 1. Thermal ellipsoid plot of the anionic moiety crystallographically characterized in $[K(2,2,2\text{-crypt})][\mathbf{1}]$. Anisotropic thermal displacement ellipsoids are pictured at the 50% probability level. Hydrogen positions were assigned idealized coordinates and are pictured as spheres of arbitrary radii. Selected bond distances (Å) and angles (deg): P1−P2, 2.102(1); P2−P3, 2.072(1); P3−C1, 1.757(3); C1−C2, 1.460(4); C2−P1, 1.737(3); C1−C3, 1.488(4); C3−C4, 1.392(4); C4−C5, 1.385(4); C5−C6, 1.379(5); C6−C7, 1.376(5); C7−N1, 1.335(4); N1−C3, 1.361(3); P1−P2−P3, 99.41(5); P2−P3−C1, 100.54(10); P3−C1−C2, 120.0(2); C1−C2−P1, 119.0(2); C2−P1−P2, 100.91(11); C2−C1−C3, 120.4(2); C1−C3−N1, 116.6(2). Torsion angle (Φ) between the pyridyl and phospholide ring: 33.1°.

collection and refinement parameters for $[K(2,2,2\text{-crypt})][\mathbf{1}]$ and all of the other crystallographically characterized species discussed herein are provided in Table 1.

The asymmetric unit of $[K(2,2,2\text{-crypt})][\mathbf{1}]$ contains a single crystallographically unique $[P_3C_2H(2\text{-}C_5H_4N)]^-$ anion in a *trans*-planar conformation accompanied by a $[K(2,2,2\text{-crypt})]^+$ cation. This species is isoelectronic with the 2-pyridylcyclopentadienyl anion, the coordination chemistry of which has been extensively studied, particularly in 1,1′-bis(2-pyridyl)-ferrocene and 1-(2-pyridyl)ferrocene type complexes.[31] Bond metric data for the triphospholide anion are in line with previously reported values for other 1,2,3-triphospholide species including the protic parent compound $[P_3C_2H_2]^-$.[12] The only notable exception is the C1−C2 bond which is longer in **1** when compared to $[P_3C_2H_2]^-$ (1.460(4) and 1.393(3) Å, respectively). While this could be interpreted as an indication of increased π-bonding between the phospholide and pyridyl rings, the inter-ring bond distance of 1.488(4) Å and the torsion angle between the rings (33.1°) are consistent with a C1−C3 single bond. It is therefore possible that the relatively long C1−C2 bond length arises due to unresolved discrete positional disorder of the phospholide in both the *trans*-(major) and *cis*-planar (minor) conformations on the same site.

The ^{31}P NMR spectrum of $[K(2,2,2\text{-crypt})][\mathbf{1}]$ reveals three multiplet resonances at 274.3, 278.3, and 293.1 ppm arising from the P1, P3, and P2 nuclei, respectively (these occur at comparable chemical shifts to $[P_3C_2H_2]^-$: 261.1 and 272.8 ppm for P1/P3 and P2, respectively). The spectrum can be simulated as an ABCX spin system. The phospholide proton (H2) is observed as a ddd multiplet in the ^{1}H NMR spectrum of $[K(2,2,2\text{-crypt})][\mathbf{1}]$ at 9.88 ppm ($^2J_{H-P}$ = 47 Hz; $^3J_{H-P}$ = 13 Hz; $^3J_{H-P}$ = 7 Hz). This resonance appears as a singlet on phosphorus decoupling. Further characterization of **1** in solution was carried out using electrospray ionization mass-spectrometry (ESI-MS). A DMF solution of $[K(2,2,2\text{-crypt})][\mathbf{1}]$ exhibited the molecular ion peak in the negative ion-mode spectrum at 195.9 Da. In the positive ion mode spectrum a mass envelope corresponding to the ion paired species $\{[K(2,2,2\text{-crypt})]_2[\mathbf{1}]\}^+$ was observed at an m/z value of 1025.8.

The optimized computed geometry of **1** (at the density functional level of theory) is in good agreement with the geometry determined by single crystal X-ray diffraction (see Supporting Information for a comparison of bond metric data). There is a moderate lengthening of the P−P and P−C bond distances in the computed structure presumably arising as an effect of the continuum dielectric model employed to simulate the presence of charge-balancing cations in the lattice. The HOMO and HOMO − 1 orbitals have pnictolide ring π-orbital character, and exhibit a single angular node. The anticipated in-phase combination of p_z orbitals of the pnictolide ring atoms mixes with π-orbitals of the pyridyl functionality affecting the composition of both the HOMO − 5 and HOMO − 9. This mixing of orbitals is also observed in the vacant LUMO, LUMO + 1, and LUMO + 2 where the π-manifolds of both the phospholide and pyridyl rings have significant contributions. These low-lying acceptor orbitals and the increased orbital overlap available with metal substituents upon coordination should make **1** a superior π-acceptor to its isolobal all-carbon analogue (*vide infra*).

Disymmetrically substituted triphospholide ligands are prochiral. Chiral metallocenes have received considerable attention as active species in asymmetric catalysis.[32] Among these systems are chiral monophospholide chelates which have the potential to act as supporting ligands in a wealth of transformations. The earliest examples of enantiomerically pure planar-chiral chelating ligand systems derived from phosphaferrocene ligands were reported independently by Ganter and Fu building on earlier fundamental studies by Mathey.[33−35] Such complexes have been demonstrated to be valuable ligand supports in a wealth of enantioselective processes.[36] These previous studies, and the good yields associated with the isolation of $[K(2,2,2\text{-crypt})][\mathbf{1}]$, prompted us to explore its coordination chemistry. A summary of these results are presented in Scheme 1.

Reaction of $[K(2,2,2\text{-crypt})][\mathbf{1}]$ with $Mo(CO)_6$ (or $Mo(py)(CO)_3$; py = pyridine) results in the isolation of the complex anion $[\{\eta^5\text{-}P_3C_2H(2\text{-}C_5H_4N)\}Mo(CO)_3]^-$ (**2**) via a simple ligand displacement reaction as evidenced by a significant upfield shift of the phospholide ^{31}P and ^{1}H NMR resonances. The resonances in the ^{31}P NMR spectrum of **2** were observed at 42.4, 70.8, and 77.6 ppm for the P2, P1, and P3 nuclei, respectively. On coordination to the molybdenum

dx.doi.org/10.1021/ic400448x | Inorg. Chem. 2013, 52, 5527−5534

Scheme 1. Reactivity of 4-(2′-Pyridyl)-1,2,3-triphospholide ($[P_3C_2H(2\text{-}C_5H_4N)]^-$; 1)[a]

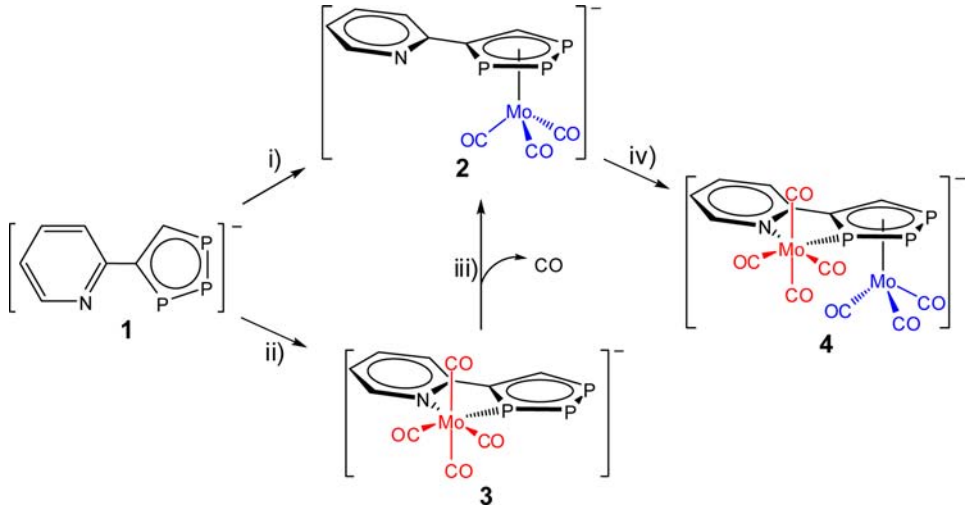

[a](i) THF, 1 equiv $Mo(py)_3(CO)_3$, 2 h, 70 °C; (ii) CH_2Cl_2, 1 equiv $Mo(COD)(CO)_4$, 48 h, 20 °C; (iii) THF, 48 h, 70 °C; (iv) CH_2Cl_2, 1 equiv $Mo(COD)(CO)_4$, 1 h, 40 °C.

metal center, the resonances for P1 and P3 shift upfield by approximately 200 ppm whereas the shift for nucleus P2 is 250.7 ppm. An upfield shift was also observed for the phospholide proton resonance (H2) which shifts to 6.84 ppm in **2** relative to 9.88 ppm in **1**. As with the ^{1}H NMR spectrum of **1**, this resonance is observed as a doublet of doublets of doublets ($^2J_{H-P}$ = 43 Hz, $^3J_{H-P}$ = 11 Hz, $^3J_{H-P}$ = 4 Hz) which collapses to a singlet on phosphorus decoupling.

Single crystal X-ray diffraction quality crystals of [K(2,2,2-crypt)][**2**] could be grown by slow diffusion of hexanes into a THF solution of the product. The product crystallizes as a racemic mixture in the centrosymmetric point group *Cmca* with several of the atoms of the anionic component lying on special crystallographic positions. In addition the 4-(2′-pyridyl)-1,2,3-triphospholide moiety exhibits positional disorder of the phospholide moiety in such a manner that both *cis*- and *trans*-planar orientations of the phospholide ring are present. Despite complications resulting from crystallographic disorder and the high symmetry space group in which the sample crystallizes, the structure is of sufficient quality to establish the composition of the anion. The anionic complex, **2**, displays a 4-(2′-pyridyl)-1,2,3-triphospholide ligand coordinated in an η^5-fashion to the molybdenum tricarbonyl moiety (see Figure 2). The disorder of the ligand moiety precludes any meaningful discussion of bond metric data although it appears that bond distances within the 1,2,3-triphospholide ligand moiety are comparable to the free ligand (see Supporting Information). The Mo−P bond distances (2.536(4)−2.616(1) Å) are approximately 0.2 Å longer than equivalent distances between the metal center and the carbon atoms of the phospholide ring (2.361(2) and 2.372(17) Å) as would be expected.

The ESI-MS spectra of DMF solutions of [K(2,2,2-crypt)][**2**] reveal mass-envelopes at 378.5 (**2**) and 1210.0 Da ($\{[K(2,2,2\text{-crypt})]_2[\mathbf{2}]\}^+$) in the negative and positive ion modes, respectively. An infrared (IR) spectrum of [K(2,2,2-crypt)][**2**] reveals three bands in the carbonyl stretching region at 1924, 1828, and 1812 cm^{-1}. These vibrational modes occur at lower wavenumbers than in the $Mo(CO)_6$ precursor (1989 cm^{-1}, T_{1u}), but at notably higher values than the all carbon analogue [K(18-crown-6)][(η^5-Cp)$Mo(CO)_3$] (1884 and 1760 cm^{-1} for the A_1 and E modes, respectively).[37,38] This finding is consistent with previous density functional theory (DFT) and photoelectron spectroscopy (PES) studies describing the increased π-acceptor capacity of cyclic phosphorus containing ligand systems relative to their carbocyclic analogues.[39] The low-lying π acceptor orbitals on phospholide ligand systems are believed to facilitate δ interactions with metal d-orbitals, hence stabilizing low-oxidation state early metal complexes such as [Ti(η^5-$P_3C_2Bu_2)_2$] or Ellis' inorganic titanocene dianion [Ti(η^5-$P_5)_2]^{2-}$.[5d,40] These interactions are apparent upon inspection of the optimized computed geometry of **2** which reveals a HOMO − 2 with significant δ-bonding character.

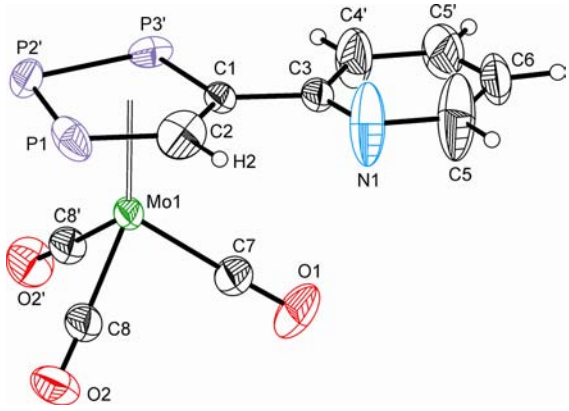

Figure 2. Thermal ellipsoid plot of the anionic moiety crystallographically characterized in [K(2,2,2-crypt)][**2**]. Anisotropic thermal displacement ellipsoids are pictured at the 50% probability level. Hydrogen positions were assigned idealized coordinates and are pictured as spheres of arbitrary radii. Symmetry operation ′: 1 − *x*, +*y*, +*z*. Crystallographic symmetry prevents the determination of the *cis*/*trans* planar isomeric form of **2** present. Selected bond distances (Å): Mo1−P1, 2.610(1); Mo1−P2, 2.616(1); Mo1−P3, 2.536(4); Mo1−C1, 2.361(2); Mo1−C2, 2.372(17); Mo1−C7, 1.964(3); Mo1−C8, 1.962(2); C7−O1, 1.157(4); C8−O2, 1.155(3); P1−P2′, 2.097(3); P2′−P3′, 2.153(5); P3′−C1, 1.772(4); C1−C2, 1.429(11); C2−P1, 1.702(17); C1−C3, 1.489(3); C3−N1/C4′, 1.340(3); N1/C4′−C5/C5′, 1.364(4); C5/C5′−C6, 1.357(5). Torsion angle (Φ) between the pyridyl and phospholide ring: 5.6°.

dx.doi.org/10.1021/ic400448x | *Inorg. Chem.* 2013, 52, 5527−5534

Reaction of [K(2,2,2-crypt)][**1**] with 1 equiv of Mo(COD)(CO)$_4$ afforded the pseudo-octahedral complex [{κ^2*P,N*-$P_3C_2H(2\text{-}C_5H_4N)$}Mo(CO)$_4$] (**3**). The reaction was monitored by $^{31}P\{^1H\}$ NMR spectroscopy revealing small upfield shifts to the phosphorus resonances of the triphospholide ligand. Three new resonances corresponding to **3** were observed at 266.6, 262.5, and 240.2 ppm (arising from P1, P3, and P2, respectively). Perhaps counterintuitively, the largest chemical shift change is not observed for the phosphorus nucleus which bonds to the metal (P3; $\Delta\delta$ = −15.8 ppm) but rather for the adjacent phosphorus atom (P2; $\Delta\delta$ = −52.9 ppm). We postulate that this is a result of opposing bonding effects which result in a negligible net change to the electron density at P3.[41] Thus, while σ-donation from the phosphorus lone pair to the metal should result in a downfield shift, this effect is compensated for by significant π-backbonding from the molybdenum(0) center to P3 and a disruption of the deshielding ring current in the aromatic phospholide ring. This change to the electron density of the π-manifold may also help to account for the shielding effect observed for the P2 resonance. This consequential degree of π-backbonding is also manifested in the bond metric data (*vide infra*). The strong π-acceptor properties of a closely related 2-(2′-pyridyl)-phosphaferrocene complex have previously been highlighted by Mathey and co-workers.[42] The loss of the lone pair electron density on P3 on complexation also results in a notable increase of the intraphospholide coupling constants involving P3 relative to **1**.

Single crystal X-ray diffraction quality crystals of [K(2,2,2-crypt)][**3**] were grown by slow diffusion of pentane into a dichloromethane solution of the compound at −35 °C (Figure 3). The crystal structure reveals a pseudo-octahedral molybdenum(0) center chelated by **1** in a κ^2-fashion through the nitrogen atom of the pyridyl ring and a triphospholide phosphorus atom. Bond metric data within the triphospholide ligand are comparable to the free ligand **1**. The Mo1−P3 and Mo−N1 bond distances are 2.483(1) and 2.323(2) Å, respectively;[43] these distances are much closer in magnitude than what would be expected on the basis of the different single bond covalent radii of phosphorus and nitrogen (Δr_{cov} = 0.30 Å).[44] The Mo−N bond distance is longer than other complexes of molybdenum(0) with pyridyl rings such as Mo(2,2′-bipyridine)(CO)$_4$ (2.249(3) and 2.240(3) Å).[45] This may be a result of the wide bite angle of the free ligand, **1**, relative to 2, 2′-bipyridine and the resulting five membered ring which results upon chelation of the metal, also manifested in an acute P−Mo−N bond angle (74.69(4)°). However, these findings are also consistent with some degree of π-backbonding between Mo1 and P3; this is additionally supported by the longer Mo1−C bond of the carbonyl that is *trans* to P3 (1.982(2) Å) compared to the ligand *trans* to N1 (1.956(2) Å). A π-acceptor ligand in the *trans* position will compete for electron density from the same metal d-orbital. Thus, a longer molybdenum carbonyl bond can be taken to be indicative of the greater π acceptor capacity of the ligand that is in a *trans* position.

Solutions of **3** were found to readily lose a carbonyl ligand on heating (70 °C, 48 h) converting to **2** in quantitative yields. Negative ion mode electrospray mass-spectrometry did reveal the presence of the parent anion in solution at an *m*/*z* value of 406.0; however, it was observed as a minor peak with the main mass envelope occurring at 378.5 Da corresponding to [{$P_3C_2H(C_5H_4N)$}Mo(CO)$_3$]$^-$ (this is unsurprising considering the 150 °C desolvation temperature used during ionization). IR spectroscopy on a Nujol mull of [K(2,2,2-crypt)][**3**] reveals four bands in the carbonyl stretching region consistent with a C_s geometry at 2004, 1895, 1879, 1828 cm^{-1}. The compositional purity of [K(2,2,2-crypt)][**3**] was established by elemental analysis and powder X-ray diffraction.

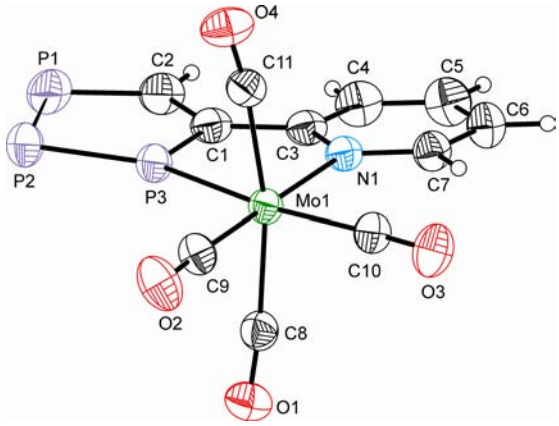

Figure 3. Thermal ellipsoid plot of the anionic moiety crystallographically characterized in [K(2,2,2-crypt)][**3**]·0.5CH_2Cl_2. Anisotropic thermal displacement ellipsoids are pictured at the 50% probability level. Hydrogen positions were assigned idealized coordinates and are pictured as spheres of arbitrary radii. Selected bond distances (Å) and angles (deg): Mo1−P3, 2.483(1); Mo1−N1, 2.323(2); Mo1−C8, 2.032(2); Mo1−C9, 1.956(2); Mo1−C10, 1.982(2); Mo1−C11, 2.047(2); C8−O1, 1.137(3); C9−O2, 1.156(3); C10−O3, 1.144(2); C11−O4, 1.138(2); P1−P2, 2.118(1); P2−P3, 2.064(1); P3−C1, 1.736(2); C1−C2, 1.403(3); C2−P1, 1.726(2); C1−C3, 1.462(3); C3−C4, 1.400(3); C4−C5, 1.367(3), C5−C6, 1.383(3); C6−C7, 1.378(3); C7−N1, 1.352(2); N1−C3, 1.369(2); N1−Mo1−P3, 74.69(4); N1−Mo1−C8, 94.34(7); N1−Mo1−C10, 93.20(7); N1−Mo1−C11, 96.38(6); P3−Mo1−C8, 88.85(6); P3−Mo1−C9, 104.09(6); P3−Mo1−C11, 87.73(5); C8−Mo1−C9, 83.87(8); C8−Mo1−C10 91.87(8); C9−Mo1−C10, 88.00(8); C9−Mo1−C11, 85.27(8); C10−Mo1−C11, 94.00(8). Torsion angle (Φ) between the pyridyl and phospholide ring: 6.4°.

Finally, we also were able to form the bimetallic species [{μ:η^5,κ^2*P,N*-$P_3C_2H(2\text{-}C_5H_4N)$}{Mo(CO)$_3$}{Mo(CO)$_4$}]$^-$ (**4**) by reaction of **2** with 1 equiv of Mo(COD)(CO)$_4$. This complex was generated *in situ* in a gastight NMR tube in CD_2Cl_2 after heating to 40 °C for one hour. The phospholide proton was observed as a ddd multiplet at 6.68 ppm which is indicative of a η^5 coordination of the ligand to a Mo(CO)$_3$ fragment (**1**, 9.88; **2**, 6.84 ; **3**, 9.51 ppm). Three multiplet resonances were also observed in the ^{31}P NMR spectrum at 119.4, 63.5, and −21.7 ppm arising from P3, P1, and P2, respectively. These shifts can be rationalized as a result of the combined electronic effects described earlier (*vide supra*) for η^5 and κ^2 coordination of the ligand in complexes **2** and **3**, respectively. Perhaps most informatively, the ^{13}C NMR spectrum of **4** reveals four resonances arising from the carbonyl ligands. The resonances at 226.2 ppm arise from the three carbonyl ligands of the Mo(CO)$_3$ moiety (*cf.*, **2**: 228.2 ppm). The remaining four carbonyl resonances 222.3, 217.7, 206.2, and 205.2 ppm are comparable to those recorded for **3** (*cf.*, **3**: 223.5, 221.1, and 207.4 ppm) and can be assigned as arising from the CO ligands that are *trans* to N, *trans* to P, and in the axial positions, respectively. Complex **4** was found to readily decompose via loss of a carbonyl under the conditions required for collection of a mass spectrum; a mass peak corresponding to **3** could be oberved in the negative ion mode (584.3 Da)

dx.doi.org/10.1021/ic400448x | *Inorg. Chem.* 2013, 52, 5527−5534

alongside a much more intense peak arising from $[4 - CO]^-$ (556.2 Da).

CONCLUSIONS

We have reported the synthesis of the first asymmetrically substituted 1,2,3-triphospholide anion isolated as a compositionally pure free ligand. The wealth of its coordination modes has been explored providing important "proof-of-concept" experiments demonstrating that η^5 metal complexes of this unique species may be used as supporting chelating ligands. Studies are currently underway trying to resolve planar chiral racemates such as **2**.

ASSOCIATED CONTENT

Supporting Information

CCDC 918948−918950 contain the supplementary crystallographic data for this paper (www.ccdc.cam.ac.uk/data_request/cif). Full experimental and computational details, NMR and ESI-MS spectra, and complete ref 27. This material is available free of charge via the Internet at http://pubs.acs.org.

AUTHOR INFORMATION

Corresponding Author

*E-mail: jose.goicoechea@chem.ox.ac.uk.

Notes

The authors declare no competing financial interest.

ACKNOWLEDGMENTS

We thank the EPSRC and the University of Oxford for financial support of this research (DTA studentship R.S.P.T.) and the University of Oxford for access to Chemical Crystallography and Oxford Supercomputing Centre facilities. We also thank Elemental Microanalysis Ltd. (Devon) for performing the elemental analyses.

REFERENCES

(1) Dillon, K. B.; Mathey, F.; Nixon, J. F. *Phosphorus: The Carbon Copy: From Organophosphorus to Phospha-organic Chemistry*, 1st ed.; John Wiley and Sons: Chichester, U.K., 1998.

(2) (a) Nixon, J. F. *Chem. Rev.* **1988**, *88*, 1327. (b) Mathey, F. *Coord. Chem. Rev.* **1994**, *137*, 1. (c) Nixon, J. F. *Chem. Soc. Rev.* **1995**, *24*, 319. (d) Le Floch, P.; Mathey, F. *Coord. Chem. Rev.* **1998**, *178*, 771. (e) Mathey, F. *Angew. Chem., Int. Ed.* **2003**, *42*, 1578. (f) Le Floch, P. *Coord. Chem. Rev.* **2006**, *250*, 627.

(3) (a) Becker, G.; Becker, W.; Knebl, R.; Schmidt, H.; Weeber, U.; Westerhausen, M. *Nova Acta Leopold.* **1985**, *59*, 1. (b) Bartsch, R.; Hitchcock, P. B.; Nixon, J. F. *J. Chem. Soc., Chem. Commun.* **1987**, 1146. (c) Cowley, A. H.; Hall, S. W. *Polyhedron* **1989**, *8*, 849. (d) Bartsch, R.; Nixon, J. F. *Polyhedron* **1989**, *8*, 2407. (e) Bartsch, R.; Nixon, J. F. *J. Organomet. Chem.* **1991**, *415*, C15.

(4) For s- and p-block complexes see: (a) Callaghan, C.; Clentsmith, G. K. B.; Cloke, F. G. N.; Hitchcock, P. B.; Nixon, J. F.; Vickers, D. M. *Organometallics* **1999**, *18*, 793. (b) Durkin, J. J.; Francis, M. D.; Hitchcock, P. B.; Jones, C.; Nixon, J. F. *J. Chem. Soc., Dalton Trans.* **1999**, 4057. (c) Francis, M. D.; Hitchcock, P. B.; Nixon, J. F. *Chem. Commun.* **2000**, 2027. (d) Francis, M. D.; Hitchcock, P. B.; Nixon, J. F.; Schnockel, H.; Steiner, J. *J. Organomet. Chem.* **2002**, *646*, 191. (e) Fish, C.; Green, M.; Jeffery, J. C.; Kilby, R. J.; Lynam, J. M.; Russell, C. A.; Willians, C. E. *Organometallics* **2005**, *24*, 5789. (f) Ionkin, A. S.; Marshall, W. J.; Fish, B. M.; Marchione, A. A.; Howe, L. A.; Davidson, F.; McEwen, C. N. *Eur. J. Inorg. Chem.* **2008**, 2386. (g) Mansell, S. M.; Green, M.; Kilby, R. J.; Murray, M.; Russell, C. A. *C. R. Chim.* **2010**, *13*, 1073.

(5) For examples of transition metal complexes see: (a) Bartsch, R.; Hitchcock, P. B.; Nixon, J. F. *J. Chem. Soc., Chem. Commun.* **1987**, 1146. (b) Bartsch, R.; Hitchcock, P. B.; Madden, T. J.; Meidine, M. F.; Nixon, J. F.; Wang, H. *J. Chem. Soc., Chem. Commun.* **1988**, 1475. (c) Black, S. J.; Francis, M. D.; Jones, C. *J. Chem. Soc., Dalton Trans.* **1997**, 2183. (d) Cloke, F. G. N.; Hanks, J. R.; Hitchcock, P. B.; Nixon, J. F. *Chem. Commun.* **1999**, 1731. (e) Heinemann, F. W.; Pritzkow, H.; Zeller, M.; Zenneck, U. *Organometallics* **2000**, *19*, 4283. (f) Clark, T.; Elvers, A.; Heinemann, F. W.; Hennemann, M.; Zeller, M.; Zenneck, U. *Angew. Chem., Int. Ed.* **2000**, *39*, 2087. (g) Cloke, F. G. N.; Hitchcock, P. B.; Nixon, J. F.; Vickers, D. M. *J. Organomet. Chem.* **2001**, *635*, 212. (h) Heinmann, F. W.; Pritzkow, H.; Zeller, M.; Zenneck, U. *Organometallics* **2001**, *20*, 2905. (i) Scheer, M.; Deng, S.; Scherer, O. J.; Sierka, M. *Angew. Chem., Int. Ed.* **2005**, *44*, 3755.

(6) Lanthanide and actinide complexes: (a) Arnold, P. L.; Cloke, F. G. N.; Hitchcock, P. B.; Nixon, J. F. *J. Am. Chem. Soc.* **1996**, *118*, 7630. (b) Deacon, G B.; Delbridge, E. E.; Fallon, G. D.; Jones, C.; Hibbs, D. E.; Hursthouse, M. B.; Skelton, B. W.; White, A. H. *Organometallics* **2000**, *19*, 1713. (c) Clentsmith, G. K. B.; Cloke, F. G. N.; Green, J. C.; Hanks, J.; Hitchcock, P. B.; Nixon, J. F. *Angew. Chem., Int. Ed.* **2003**, *42*, 1038. (d) Clentsmith, G. K. B.; Cloke, F. G. N.; Francis, M. D.; Hanks, J. R.; Hitchcock, P. B.; Nixon, J. F. *J. Organomet. Chem.* **2008**, *693*, 2287.

(7) Baudler, M.; Hahn, J. *Z. Naturforsch., B: Chem. Sci.* **1990**, *45b*, 1139.

(8) (a) Scherer, O. J.; Hilt, T.; Wolmershäuser, G. *Angew. Chem., Int. Ed.* **2000**, *39*, 1425. (b) Deng, S.; Schwarzmaier, C.; Eichhorn, C.; Scherer, O.; Wolmershäuser, G.; Zabel, M.; Scheer, M. *Chem. Commun.* **2008**, 4064. (c) Deng, S.; Schwarzmaier, C.; Zabel, M.; Nixon, J. F.; Timoshkin, A. Y.; Scheer, M. *Organometallics* **2009**, *28*, 1075.

(9) Maigrot, N.; Sierra, M.; Charrier, C.; Mathey, F. *Bull. Soc. Chim. Fr.* **1994**, *131*, 397.

(10) García, F.; Less, R. J.; Naseri, V.; McPartlin, M.; Rawson, J. M.; Sancho Tomas, M.; Wright, D. S. *Chem. Commun.* **2008**, 859.

(11) Butts, C. P.; Green, M.; Hooper, T. N.; Kilby, R. J.; McGrady, J. E.; Pantazis, D. A.; Russell, C. A. *Chem. Commun.* **2008**, 856.

(12) Turbervill, R. S. P.; Goicoechea, J. M. *Chem. Commun.* **2012**, *48*, 6100.

(13) Santandrea, R. P.; Mensing, C.; von Schnering, H.-G. *Thermochim. Acta* **1986**, *98*, 301.

(14) Pearson, A. J.; Schoffers, E. *Organometallics* **1997**, *16*, 5365.

(15) Tekkaya, A.; Kayran, C.; Özkar, S.; Kreiter, C. G. *Inorg. Chem.* **1994**, *33*, 2439.

(16) Cosier, J.; Glazer, A. M. *J. Appl. Crystallogr.* **1986**, *19*, 105.

(17) *CrysAlisPro, Version 1.171.35.8*; Agilent Technologies.

(18) (a) Sheldrick, G. M. *Acta Crystallogr.* **2008**, *A64*, 112. (b) Sheldrick, G. M. *Acta Crystallogr., Sect. A* **1990**, *46*, 467. (c) Sheldrick, G. M. *SHELX97, Programs for Crystal Structure Analysis (Release 97−2)*; University of Göttingen: Göttingen, Germany, 1998.

(19) NMR spectra simulated using: Budzelaar, P. H. M. *gNMR v5.0*; IvorySoft, 1995−2006.

(20) (a) te Velde, G.; Bickelhaupt, F. M.; Baerends, E. J.; Fonseca Guerra, C.; van Gisbergen, S. J. A.; Snijders, J. G.; Ziegler, T. *J. Comput. Chem.* **2001**, *22*, 931. (b) Fonseca Guerra, C.; Snijders, J. G.; te Velde, G.; Baerends, E. J. *Theor. Chem. Acc.* **1998**, *99*, 391. (c) *ADF 2008.01*; SCM, Theoretical Chemistry, Vrije Universiteit: Amsterdam, The Netherlands, http://www.scm.com.

(21) Parr, R. G.; Yang, W. In *Density Functional Theory of Atoms and Molecules*; Oxford University Press: Oxford, 1989.

(22) Vosko, S. H.; Wilk, L.; Nusair, M. *Can. J. Phys.* **1980**, *58*, 1200.

(23) (a) Becke, A. D. *Phys. Rev. A* **1988**, *38*, 3098. (b) Perdew, J. P. *Phys. Rev. B* **1986**, *33*, 8822.

(24) (a) van Lenthe, E.; Baerends, E. J.; Snijders, J. G. *J. Chem. Phys.* **1993**, *99*, 4597. (b) van Lenthe, E.; Baerends, E. J.; Snijders, J. G. *J. Chem. Phys.* **1994**, *101*, 9783. (c) van Lenthe, E.; Ehlers, A.; Baerends, E. J. *J. Chem. Phys.* **1999**, *110*, 8943.

(25) Klamt, A.; Schüürmann, G. *J. Chem. Soc., Perkin Trans. 2* **1993**, 799.

(26) Versluis, L.; Ziegler, T. *J. Chem. Phys.* **1988**, *88*, 322.

(27) Frisch, M. J.; et al. *Gaussian 09, Revision A.02*; Gaussian, Inc.: Wallingford, CT, 2009.
(28) (a) Becke, A. D. *J. Chem. Phys.* **1993**, *98*, 5648. (b) Perdew, J. P. In *Electronic Structure of Solids '91*; Ziesche, P., Eschrig, H., Eds.; Akademie Verlag: Berlin, 1991; p 11.
(29) (a) Krishnan, R.; Binkley, J. S.; Seeger, R.; Pople, J. A. *J. Chem. Phys.* **1980**, *72*, 650. (b) Blaudeau, J.-P.; McGrath, M. P.; Curtiss, L. A.; Radom, L. *J. Chem. Phys.* **1997**, *107*, 5016. (c) Clark, T.; Chandrasekhar, J.; Schleyer, P. v. R. *J. Comput. Chem.* **1983**, *4*, 294.
(30) Dobbs, K. D.; Hehre, W. J. *J. Comput. Chem.* **1987**, *8*, 880.
(31) (a) Yoshida, T.; Tani, K.; Yamagata, T.; Tatsuno, Y.; Saito, T. *J. Chem. Soc., Chem. Commun.* **1990**, 292. (b) Tani, K.; Mihana, R.; Yamagata, T.; Saito, T. *Chem. Lett.* **1991**, *20*, 2047. (c) Delis, J. G. P.; van Leeuwen, P. W. N. M.; Vrieze, K.; Veldman, N.; Spek, A. L.; Fraanje, J.; Goubitz, K. *J. Organomet. Chem.* **1996**, *514*, 125. (d) Hijazi, A.; Djukic, J.-P.; Pfeffer, M.; Ricard, L.; Kyritsakas-Gruber, N.; Raya, J.; Bertani, P.; de Cian, A. *Inorg. Chem.* **2006**, *45*, 4589. (e) Hijazi, A.; Djukic, J.-P.; Allouche, L.; de Cian, A.; Pfeffer, M.; Le Goff, X.-F.; Ricard, L. *Organometallics* **2007**, *26*, 4180. (f) Štěpnička, P.; Schulz, J.; Klemann, T.; Siemeling, U.; Císařová, I. *Organometallics* **2010**, *29*, 3187. (g) Siemeling, U.; Klemann, T.; Bruhn, C.; Schulz, J.; Štěpnička, P. *Dalton Trans.* **2011**, *40*, 4722. (h) Siemeling, U.; Klemann, T.; Bruhn, C.; Schulz, J.; Štěpnička, P. *Z. Anorg. Allg. Chem.* **2011**, *637*, 1824. (i) Suenkel, K.; Weigand, S. *Inorg. Chim. Acta* **2011**, *370*, 224.
(32) *Chiral Ferrocenes in Asymmetric Catalysis*; Dai, L. X., Hou, X.-L., Eds.; Wiley-VCH: Weinheim, 2010.
(33) Ganter, C.; Glinsböckel, C.; Ganter, B. *Eur. J. Inorg. Chem.* **1998**, 1163.
(34) Qiao, S.; Fu, G. C. *J. Org. Chem.* **1998**, *63*, 4168.
(35) Roman, E.; Leiva, A. M.; Casasempere, M. A.; Charrier, C.; Mathey, F.; Garland, M. T.; le Marouille, J.-Y. *J. Organomet. Chem.* **1986**, *309*, 332.
(36) Fu, G. C. *Acc. Chem. Res.* **2006**, *39*, 853 and references therein.
(37) Brown, T. L.; Darensbourg, D. J. *Inorg. Chem.* **1967**, *6*, 971.
(38) Haines, R. J.; Nolte, C. R. *J. Organomet. Chem.* **1970**, *24*, 725.
(39) (a) Gleiter, R.; Hyla-Kryspin, I.; Binger, P.; Regitz, M. *Organometallics* **1992**, *11*, 177. (b) Cloke, F. G. N.; Green, J. C.; Hanks, J. R.; Nixon, J. F.; Suter, J. L. *J. Chem. Soc., Dalton Trans.* **2000**, 3534. (c) Bartsch, R.; Cloke, F. G. N.; Green, J. C.; Matos, R. M.; Nixon, J. F.; Suffolk, R. J.; Suter, J. L.; Wilson, D. J. *J. Chem. Soc., Dalton Trans.* **2001**, 1013.
(40) Urnèžius, E.; Brennessel, W. W.; Cramer, C. J.; Ellis, J. E.; Schleyer, P. v. R. *Science* **2002**, *295*, 832.
(41) For an overview of ^{31}P NMR spectroscopy see: Kühl, O. *Phosphorus-31 NMR Spectroscopy: A Concise Introduction for the Synthetic Organic and Organometallic Chemist*, 1st ed.; Springer-Verlag: Berlin/Heidelberg, 2008.
(42) Deschamps, B.; Richard, L.; Mathey, F. *J. Organomet. Chem.* **1997**, *548*, 17.
(43) A survey of the Cambridge Structural Database (CSD; version 5.33, August 2012 update) reveals that while the Mo−P bond distance in **3** (2.483(1) Å) is close to the average value for the 2546 reported complexes containing a Mo−P bond (2.496 Å; mean SE 0.001; sample SD 0.068), the Mo−N bond distance (2.323(2) Å) is notably longer when compared to the 4259 entries containing an Mo−N bond (2.168 Å; mean SE 0.001; sample SD 0.148).
(44) Pyykkö, P.; Atsumi, M. *Chem.—Eur. J.* **2009**, *15*, 186.
(45) Braga, S. S.; Coelho, A. C.; Gonçalves, I. S.; Paz, F. A. A. *Acta Crystallogr., Sect. E* **2007**, *63*, m780.